Terahertz detection of chemicals through zeonex fiber material

M. B. Hossain[a], K. A. J. Alsalem[b], K. Ahmed[c,d,*], F. M. Bui[c], S. M. Ibrahim[e], S. K. Patel[f]
[a]*Faculty of Engineering, the University of Sydney, NSW-2006, Australia*
[b]*Department of Medical Instrumentation Engineering Techniques, Al-Kunooze University College, Basra, Iraq*
[c]*Department of Electrical and Computer Engineering, University of Saskatchewan, Saskatoon, SK S7N 5A9, Canada*
[d]*Group of Bio-photomatiχ, Department of Information and Communication Technology, Mawlana Bhashani Science and Technology University, Santosh, Tangail-1902, Bangladesh*
[e]*Department of Biochemistry, College of Science, King Saud University, P.O. Box 2455, Riyadh 11451, Saudi Arabia*
[f]*Computer Engineering Department, Marwadi University 360003, Gujarat, India*

A PCF sensor is proposed for chemical (e.g., glycerol, acetic acid, and water) sensing through Zeonex fiber material. We investigate relative sensitivity, effective are, effective material loss, and confinement loss to analyze the sensor performance. The proposed sensor offers the relative sensitivity of almost 97.7% for glycerol, 96.25% for acetic acid, 95.28% for water at frequency 3.5 THz. In addition, the sensor possesses small effective material loss and tiny confinement loss that are important characteristics of an efficient chemical sensor. Furthermore, the modern fabrication techniques are well fitting for the fabrication of the presented sensor.

(Received January 23, 2023; Accepted April 13, 2023)

Keywords: Zeonex material, PCF, Chemical sensor, Terahertz

1. Introduction

Glycerol, acetic acid, and water are three of the mostly used liquids or chemicals in the chemical industries nowadays. These chemicals have numerous uses in our daily household jobs. However, these chemicals can be hurtful consequences to human health if they are used improperly. For example, Glycerol may cause serious damage to red blood cells of human blood when improper amount of it is used for medication. Also, the inappropriate use of Acetic acid may injure various human internal organs, human skin, and eyes. In addition, water, the most plenteous liquid in earth is mostly used in industry among all the liquids, but if it is not properly used or discharged, it may cause water pollution and that may imbalance the ecosystem. Therefore, precious sensing of these chemicals is worthy. Up to date, several techniques have been reported to sense various chemicals [1-6]. However, these techniques are not enough efficient. So, to obtain an efficient sensor for chemical sensing, still research is going on.

Recently, Photonic Crystal Fiber (PCF) has attracted the attention of academia as well as industry for its unique possibility in optical sensing field [7- 13]. PCF sensors are seemed appealing among researchers for their incredible characteristics, for instance, small size, sensor design flexibility, and robustness. In case of PCF sensor, the sensing characteristics namely relative sensitivity (RS), effective area (EA), effective material loss (EML), confinement loss, and-so-on, can be engineered by tuning the core-clad hole size, shape, and position, etc. Numerous research works have already been published to sense various chemicals, or liquids [7-10]. Earlier silica glass was vastly preferred as optical media while very recently Teflon, Topas and Zeonex have become preferable to the researchers especially in terahertz (THz) regime [10-15]. Among all

* Corresponding author: k.ahmed@usask.ca
https://doi.org/10.15251/DJNB.2023.182.511

of them, Zeonex has attended more demand for its extraordinary optical properties, for instance, low absorption loss (only 0.2 cm^{-1} in THz frequency range), better light confinement, and on top of these it offers constant refractive index (1.53) within the THz regime [10-12]. So, for the chemical or liquid sensing purpose, Zeonex is one of the best candidates especially when the sensor is operated in THz regime [10-12].

In recent times, numerous research articles have been published on chemical sensing through PCF [16-23]. Ademgil and Shyqyri proposed a liquid sensor with a RS of 23.8% [18]. Ademgil presented an octagonal PCF sensor to sense three liquids (water, ethanol, and benzyne), and that sensor offered the RS of around 25.1% [19]. Asaduzzaman and his research group reported a PCF based ethanol sensor with a RS of around 29.3% [20]. Arif et al. suggested another liquid sensor with a RS of 48.5% [21]. Later on, for ethanol detection, Asaduzzaman et al. found the RS of approximately 49.2% with another sensor structure [22]. Afterwards, Podder et al. proposed another PCF sensor to detect Ethanol and they achieved a RS of 54% [23]. Furthermore, Arif et al. reported a liquid sensor with the RS of 53.4% [24]. Paul et al. proposed a folded cladding porous shaped PCF sensor with a RS of 64.2% with tiny confinement loss (CL) [25].

Recently, the researchers have experienced that the performance of PCF based analyte sensors is much better while they are operated in THz regime [26-35]. Sultana et al. has published an article on THz alcohol sensor, and they found the relative sensitivity of 68.9% with high birefringence (0.0176) [26]. Al-Shafi and Sen have proposed an octagonal core chemical sensor and they attained the RS of around 78% [27]. Ahmed et al. reported a blood component sensor with a significant improvement in sensitivity and they found 80.9% RS with negligible CL [28]. Islam and his research group have reported a THz PCF sensor to sense three chemicals namely water, ethanol, and benzene and that sensor model has offered a sensitivity of approximately 85.7% [29]. Later on, the same research group presented a cyanide sensor with the RS of almost 85.8% [30]. Hossain et al. also reported a cyanide sensor in the terahertz regime, and they achieved a sensitivity of almost 88.5% [31]. In this article, a rectangular core PCF model is proposed for sensing glycerol, acetic acid, and water and the possible fabrication techniques for this proposed sensor have also been reported.

2. Sensor model and fabrication opportunities

COMSOL Multiphysics v5.3 is used to design and simulate the presented sensor model. The presented sensor structure is shown in Figure 1. Zeonex is used as fiber material and water is chosen as analyte for this work. The sensor structure includes total fifteen rectangular holes where the central rectangular hole is used as core region and another fourteen rectangular holes surrounded the central core hole are taken as clad region. The length of core hole, L = 480 μm whereas the width of the core hole, W= 380 μm. In the cladding region, the width of all rectangles (R1-R14) is L μm whereas, the length of R1 and R2 is 4.4*W μm, the length of R3, R4, R5 and R6 is 4.4*W μm, the length of R7, R8, R9 and R10 is 3.55*W μm, and the length of R11, R12, R13 and R14 is 2*W μm. A perfectly match layer is applied just next to the cladding region, and perfectly matched layer (PML) absorbs the outgoing light waves. The PML is around 9% of the radius of the fiber material and Zeonex is also used as PML layer. Once the sensor structure is attained then the mesh analysis is accomplished by selecting the Physics-controlled mesh and the "finer" mesh is chosen in this work. The complete mesh consists of 86448 domain elements and 6024 boundary elements. The mesh view of the proposed sensor is presented in Figure 2. After accomplishing the mesh analysis, the sensor is simulated for specific chemical and Figure 3 shows the mode power distribution of the sensor for different chemicals.

Initially the PCF fabrication technique was limited to the stack and draw method [36]. However, the stack and draw method was not able to fabricate different complex PCF structures [37]. Therefore, currently numerous PCF fabrication techniques have been reported, for example, drilling [38], sol-gel [39], extrusion [40] and 3D-printing [41]. Among these techniques, the sol-gel method is useful for the fabrication of circular holes while the 3D-printing and extrusion techniques potentially execute the fabrication of square, rectangular, and elliptical holes. In addition, it has been reported that the Max Plank Institute has already accomplished the fabrication

of rectangular holes [42]. Since the presented sensor model consists of rectangular holes, it can be fabricated by using the 3D-printing and extrusion techniques.

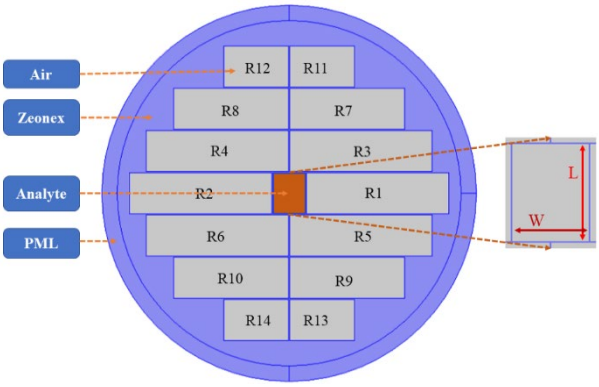

Fig. 1. The PCF sensor structure.

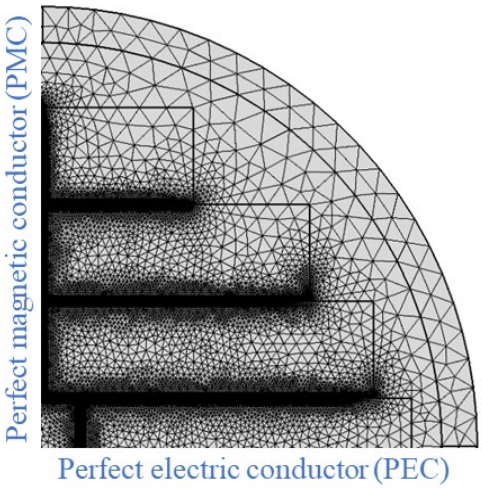

Fig. 2. Mesh view of PCF sensor.

3. Results and discussions

Aimed to investigate the optimal outcomes of the sensor, the core-clad holes size is retained affixed, while the strut (the spacing between any two consecutive rectangular holes) is varied. The sensing properties of sensor are analyzed for three different struts (14 µm, 9 µm, and 5 µm) and for three different analytes (water, acetic acid, and glycerol). To sense the sensor performance for different analytes, they are given to the core of the sensor and the investigation is accomplished for the operating frequency of 1.2 THz to 3.6 THz.

It is well known that the RS of the sensor represents the sensing capacity of any refractive index (RI)-based PCF sensors. The key instigator of sensing is the RS which can be quantified as follows [24, 30, 31]:

$$r = \frac{n_{analyte}}{n_{eff}} \times P \tag{1}$$

where, $n_{analyte}$ denotes the refractive index of analyte that is 1.47 for glycerol, 1.37 for acetic acid, 1.33 for water. Also, n_{eff} presents the effective mode index of the sensor. Hence, P denotes

the core power fraction and it is measured in terms of the integration of the electric field (E) and magnetic field (H) as follows [24, 30, 31]:

$$P = \frac{\int_{analyte} Re(E_x H_y - H_x E_y) dxdy}{\int_{total} Re(E_x H_y - H_x E_y) dxdy} \times 100 \quad (2)$$

The RS of the sensor largely depends on the core power fraction that is obtained from Eq. (2). The higher the core power fraction focuses the higher the RS. The core power fraction of the sensor depends on the core size as well as the spacing between any two holes (strut).

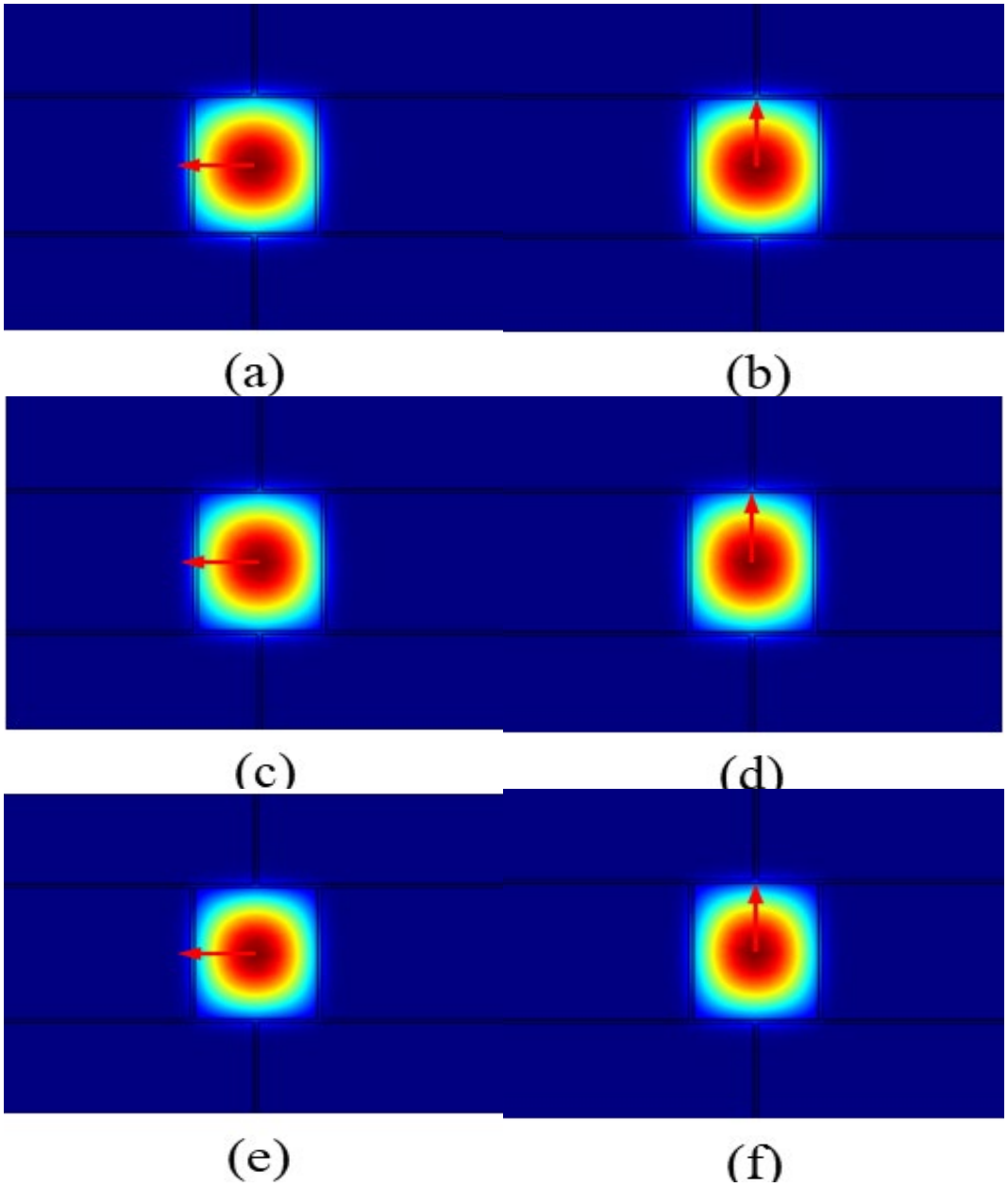

Fig. 3. Mode power distribution for a) water, x polarization; b) water, y polarization; c) acetic acid, x polarization; d) acetic acid, y polarization; e) glycerol, x polarization; f) glycerol, y polarization.

Figure 4 shows the core power fraction vs core width variation. It is found that the core power fraction is increasing for a moderate value of core width (up to 380 um). Again, keeping the

core size fixed, the strut width is changed in order to realize the sensor performance. For each chemical, the strut of the sensor is changed for three times. Then we also change the chemical for each strut and higher core power fraction is observed for the chemical with higher refractive index (glycerol). The core power fraction vs strut width variation is shown in Figure 5. The higher core power fraction is found to increase very fast with increasing operating frequency for each chemical. After a moderate value of the operating frequency the change in core power fraction is very tiny. Figures 6-11 show the RS of the sensor for three different chemicals. The sensitivity is found to increase with increasing operating frequency because the core power fraction is larger for higher frequency. Also, for the chemical with higher RI (glycerol) offers higher sensitivity. The cause is that the light confinement in core with higher indexed chemical (glycerol>acetic acid>water) is better. Besides, slightly higher relative sensitivity is found in y polarization and the reason behind this is that effective refractive index (n_{eff}) comes to be smaller in y polarization mode when compared with x polarization mode for any specific operating frequency for this PFC sensor. The relative sensitivity is found almost 96.03% for glycerol, 92.45% for acetic acid, 89.05% for water in x polarization and it is found almost 96.4% for glycerol, 92.9% for acetic acid, 89.6% for water in y polarization while strut is 14 um and operating frequency is 3.5 THz. The relative sensitivity is found almost 97.35% for glycerol, 95.75% for acetic acid, 94.7% for water in x polarization and it is found almost 97.7% for glycerol, 96.25% for acetic acid, 95.28% for water in y polarization while strut is 9 um and operating frequency is 3.5 THz. The relative sensitivity is found almost 98.2% for glycerol, 97.35% for acetic acid, 96.78% for water in x polarization and it is found almost 98.5% for glycerol, 97.78% for acetic acid, 97.4% for water in y polarization while strut is 5 um and operating frequency is 3.5 THz.

The sensor structure that has the strut of 9 μm is considered as “optimal” design. The reason is that this design affords high sensitivity and there is sufficient spacing between any two adjacent holes which is an important issue for the fabrication of the PCF sensor.

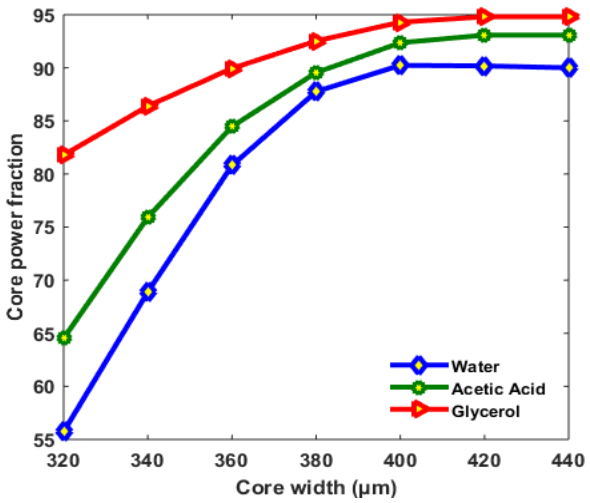

Fig. 4. Core power fraction vs core width for different chemicals at strut=14 μm and operating frequency is 2 THz.

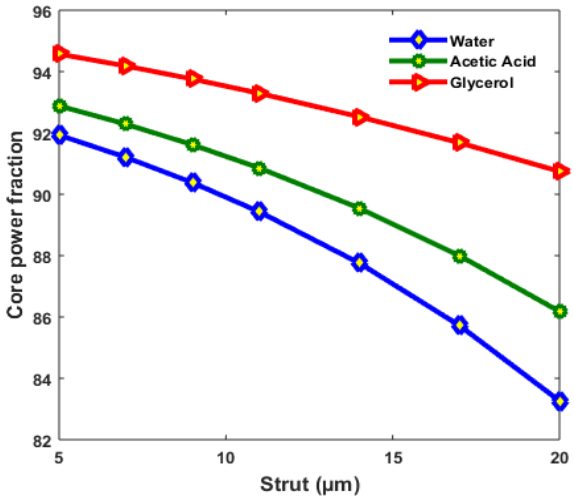

Fig. 5. Core power fraction vs strut width for different chemicals at core width=380 μm and operating frequency is 2 THz.

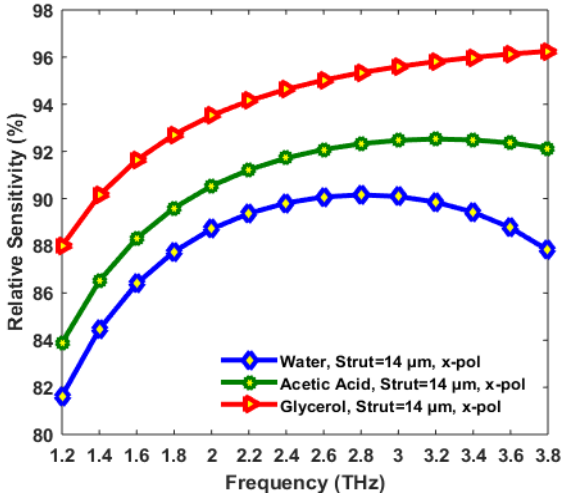

Fig. 6. Sensitivity of PCF sensor for different chemicals in x direction while strut=14 μm.

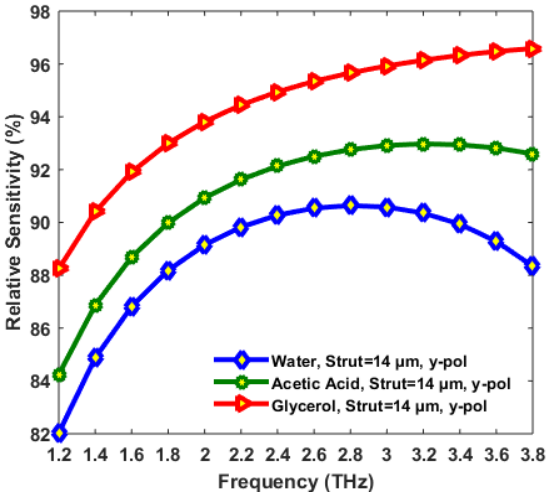

Fig. 7. Sensitivity of PCF sensor for different chemicals in y direction while strut=14 μm.

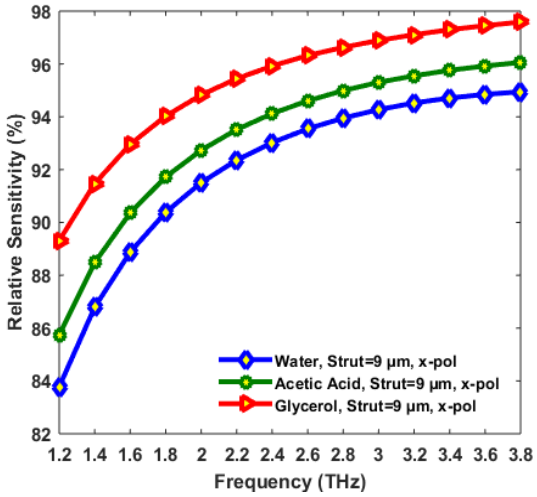

Fig. 8. Sensitivity of PCF sensor for different chemicals in x direction while strut=9 µm.

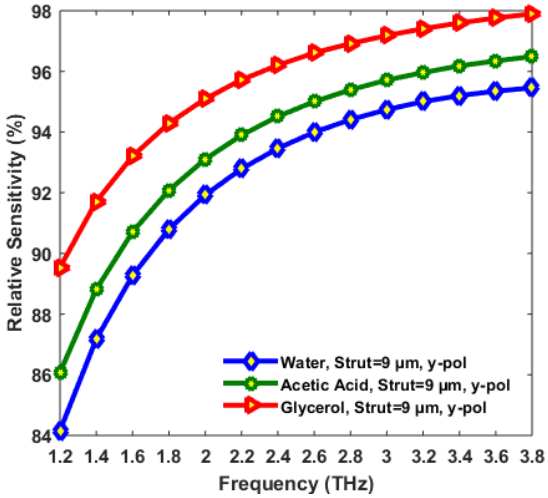

Fig. 9. Sensitivity of PCF sensor for different chemicals in y direction while strut=9 µm.

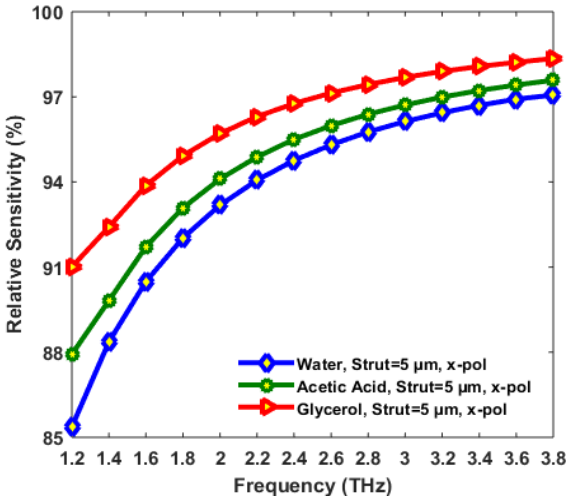

Fig. 10. Sensitivity of PCF sensor for different chemicals in x direction while strut=5 µm.

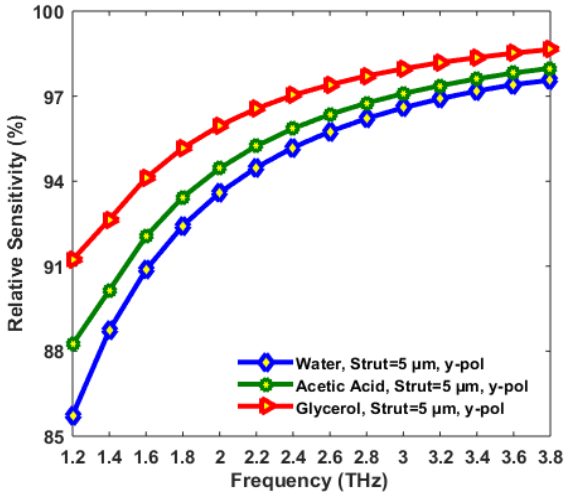

Fig. 11. Sensitivity of PCF sensor for different chemicals in y direction while strut=5 µm.

After having the optimal sensor structure, we also analyze the EA, EML, and CL profile for this sensor. In the case of EA, EML and CL, we haven't found any significant asymmetry and for this reason in this work, we have presented these results in one axis (i.e., x axis). The area of any sensor where the light wave confines effectively is called EA. It can be analyzed as follows [24]:

$$EA = \frac{[\int I(y) y dy]^2}{[\int I(y)^2 dy]^2} \tag{3}$$

where $I(y)$ denotes the transverse electric field intensity. Figure 12 shows the EA profile of this sensor for various operating frequency. Comparatively high EA is found for the analyte with lower refractive index (water) and the reason behind it is for the lower indexed analyte (water), the light wave through the core region goes spread-out. The EA of this sensor is found around 1.045×10^5 µm^2 for water, 1.040×10^5 µm^2 for acetic acid, and 1.012×10^5 µm^2 for glycerol at operating frequency 3.5 THz.

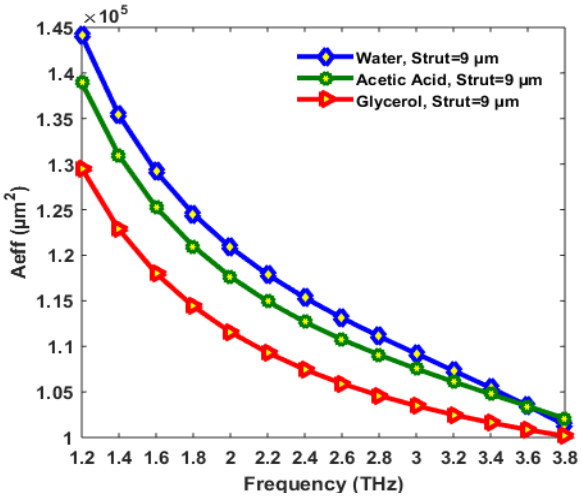

Fig. 12. Effective Area of PCF sensor for different chemicals.

Effective Material Loss is a performance limiting factor of a PCF sensor. The performance of the sensor is improved by a reduced EML. The EML of the proposed sensor can be calculated as follows [30, 31]:

$$EML = \sqrt{\frac{\epsilon_0}{\mu_0}} \times \left(\frac{\int_{material} n_{material} |E|^2 \alpha_{material} dA}{\left| \int_{all} P_z dA \right|} \right) \tag{4}$$

where ϵ_0 denotes permittivity, and μ_0 denotes permeability in free space. The parameter, $n_{material}$ is the refractive index of Zeonex and $\alpha_{material}$ is the bulk absorption loss of Zeonex. Also, P_z represents the pointing vector in z direction and $\mathrm{P_z} = \frac{1}{2}(\mathrm{E} \times \mathrm{H}^*)\hat{z}$ where, E denotes the electric filed, and H^* stands for the complex conjugate of the magnetic field.

Figure 13 shows the EML profile of the proposed sensor. The EML of the sensor goes higher for the higher operating frequency and the reason is theoretically realized in ref. [35]. Again, for higher indexed analyte (glycerol), the EML is higher. The EML is found around 0.0103 cm^{-1} for water, 0.0113 cm^{-1} for acetic acid, 0.0130 cm^{-1} for glycerol at operating frequency 3.5 THz.

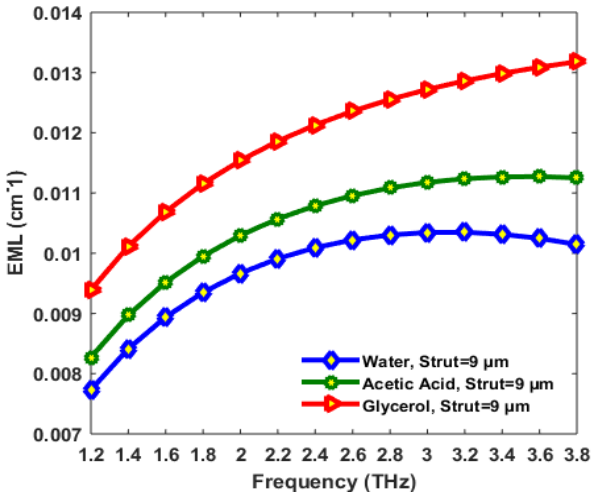

Fig. 13. Effective Material Loss of PCF sensor for different chemicals.

Confinement loss (CL) also limits the PCF sensor performance. The confinement loss depends on the operating frequency (f), the speed of light (c), and the imaginary value of effective RI of the sensor. It can be calculated as follows [30, 31, 34]:

$$CL = \frac{4\pi f}{c} \times Im(n_{eff}) \tag{5}$$

The CL of this sensor is shown in Figure 14. The CL decreases as operating frequency is increased. For increasing frequency, the light power confines strongly within the core region (through chemicals) that offers lower confinement loss. Again, for higher indexed chemical (glycerol), the CL becomes lower. The CL is found only 2.52×10^{-14} cm^{-1} for water, 1.12×10^{-14} cm^{-1} for acetic acid, and 0.55×10^{-14} cm^{-1} for glycerol at frequency 3.5 THz.

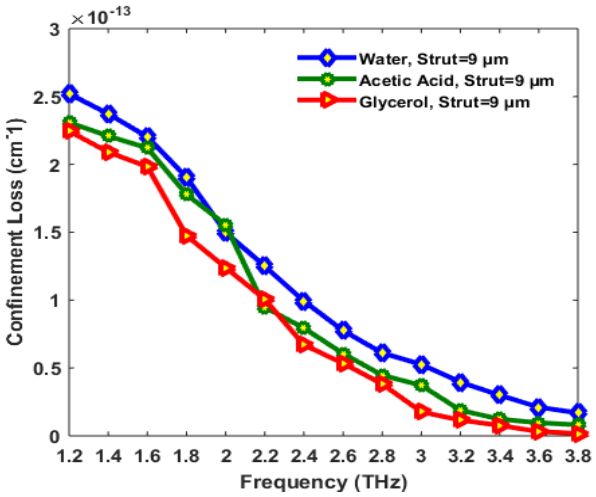

Fig. 14. Confinement loss of PCF sensor for different chemicals.

Now, we present the comparative study of sensing properties of recently published chemical sensors in Table 1.

Table 1. Sensing properties comparison between the proposed sensor and related previous works.

Ref.	Operating Region	RS	EA	EML	CL
[19]	1.5 μm	25.1%	----------	----------	1.32 ×10^{-9} cm^{-1}
[21]	1.33 μm	48.5%	----------	----------	1 ×10^{-9} cm^{-1}
[24]	1.3 μm	53.4%	3.93 um^2	----------	3.7×10^{-11} cm^{-1}
[27]	1.0 THz	78.06%	----------	----------	3.02 ×10^{-8} cm^{-1}
[30]	2.0 THz	85.80%	----------	0.023 cm^{-1}	1.6×10^{-9} cm^{-1}
[31]	1.3 THz	88.50%	---------	0.005 cm^{-1}	1.2×10^{-13} dB/cm
Proposed sensor	3.5 THz	97.7%	1.012×10^5 μm^2	0.0130 cm^{-1}	2.52×10^{-14} cm^{-1}

4. Conclusions

A PCF sensor is proposed where both the core and the cladding region are consisted of rectangular holes. Here, we instigate the sensing performance of the sensor in Terahertz regime (from 1.2 THz to 3.8 THz). Glycerol, acetic acid, and water are preferred as sensing analytes and Zeonex is taken as fiber material for this work. In an effort to inspect the functioning of the sensor, we enumerate the sensing characteristics of PCF such as RS, EA, EML, and CL. Our proposed sensor provides the RS of almost 97.7% for glycerol, 96.25% for acetic acid, 95.28% for water at operating frequency 3.5 THz. In addition, the EA of 1.045×10^5 μm^2 for water, 1.040×10^5 μm^2 for acetic acid, and 1.012×10^5 μm^2 for glycerol are availed by our proposed sensor at operating frequency 3.5 THz. Besides, the sensor offers minor EML and a little CL which reveals our

proposed sensor as an efficient chemical sensor. Additionally, the modern fabrication techniques are congenial for the fabrication of the presented chemical sensor.

Funding

This work was supported in part by funding from the Natural Sciences and Engineering Research Council of Canada (NSERC).

Acknowledgements

This work was supported by Researchers Supporting Project number (RSP2023R100), King Saud University, Riyadh, Saudi Arabia

References

[1] Y. G. Timofeyenko, J. J. Rosentreter, S. Mayo, Analytical chemistry 79(1), 251 (2007); https://doi.org/10.1021/ac060890m

[2] J. Wu, L. Wang, Q. Wang, L. Zou, B. Ye, Talanta 150, 61 (2016); https://doi.org/10.1016/j.talanta.2015.12.026

[3] D. Cleveland, M. Carlson, E. D. Hudspeth, L. E. Quattrochi, K. L. Batchler, S. A. Balram, R. G. Michel, Spectroscopy Letters 40(6), 903 (2007); https://doi.org/10.1080/00387010701525638

[4] M. F. Isaac-Lam, International Journal of Spectroscopy (2016); https://doi.org/10.1155/2016/2526946

[5] X. Jiaqiang, C. Yuping, C. Daoyong, S. Jianian, Sensors and Actuators B: Chemical 113(1), 526 (2006); https://doi.org/10.1016/j.snb.2005.03.097

[6] L. V. Shkotova, A. P. Soldatkin, M. V. Gonchar, W. Schuhmann, S. V. Dzyadevych, Materials Science and Engineering: C 26(2), 411 (2006); https://doi.org/10.1016/j.msec.2005.10.031

[7] T. Huang, Plasmonics 12(3), 583 (2017); https://doi.org/10.1007/s11468-016-0301-7

[8] E. Arik, C. Koral, H. Altan, O. Esentürk, In 2013 38th International Conference on Infrared, Millimeter, and Terahertz Waves (IRMMW-THz) (pp. 1-1), IEEE (2013, September).

[9] M. B. Hossain, E. Podder, A. A. M. Bulbul, H. S. Mondal, Optical Fiber Technology 54, 102102 (2020); https://doi.org/10.1016/j.yofte.2019.102102

[10] G. Woyessa, A. Fasano, C. Markos, A. Stefani, H. K. Rasmussen, O. Bang, Optical Materials Express 7(1), 286 (2017); https://doi.org/10.1364/OME.7.000286

[11] https://www.zeonex.com. Accessed on 27th July, 2022.

[12] J. Anthony, R. Leonhardt, A. Argyros, M. C. Large, JOSA B 28(5), 1013 (2011); https://doi.org/10.1364/JOSAB.28.001013

[13] M. S. Islam, J. Sultana, S. Rana, M. R. Islam, M. Faisal, S. F. Kaijage, D. Abbott, Optical Fiber Technology 34, 6 (2017); https://doi.org/10.1016/j.yofte.2016.11.014

[14] G. Emiliyanov, P. E. Høiby, L. H. Pedersen, O. Bang, Sensors 13(3), 3242 (2013); https://doi.org/10.3390/s130303242

[15] A. Y. Pawar, D. D. Sonawane, K. B. Erande, D. V. Derle, Drug invention today 5(2), 157 (2013); https://doi.org/10.1016/j.dit.2013.03.009

[16] E. Podder, M. Hossain, R. H. Jibon, A. A. M. Bulbul, H. S. Mondal, Frontiers of Optoelectronics 12(4), 372 (2019); https://doi.org/10.1007/s12200-019-0903-8

[17] B. K. Paul, M. Islam, K. Ahmed, S. Asaduzzaman, Photonic Sensors 7(2), 123 (2017); https://doi.org/10.1007/s13320-017-0376-6

[18] H. Ademgil, S. Haxha, Sensors 15(12), 31833 (2015); https://doi.org/10.3390/s151229891

[19] H. Ademgil, Optik 125(20), 6274 (2014); https://doi.org/10.1016/j.ijleo.2014.08.018

[20] S. Asaduzzaman, K. Ahmed, Optica Applicata 47(1), (2017).
[21] M. Arif, F. Huq, K. Ahmed, S. Asaduzzaman, M. Azad, A. Kalam, Photonic Sensors 6(3), 279 (2016); https://doi.org/10.1007/s13320-016-0323-y
[22] S. Asaduzzaman, K. Ahmed, T. Bhuiyan, T. Farah, SpringerPlus 5(1), 1 (2016); https://doi.org/10.1186/s40064-016-2415-y
[23] E. Podder, M. Hossain, A. A. M. Bulbul, H. S. Mondal, In Proceedings of International Joint Conference on Computational Intelligence (pp. 175-182), Springer, Singapore (2020); https://doi.org/10.1007/978-981-13-7564-4_15
[24] M. F. H. Arif, M. J. H. Biddut, Sensing and Bio-Sensing Research 12, 8 (2017); https://doi.org/10.1016/j.sbsr.2016.11.003
[25] B. K. Paul, K. Ahmed, S. Asaduzzaman, M. S. Islam, Sensing and Bio-Sensing Research 12, 36 (2017); https://doi.org/10.1016/j.sbsr.2016.11.005
[26] J. Sultana, M. S. Islam, K. Ahmed, A. Dinovitser, B. W. H. Ng, D. Abbott, Applied optics 57(10), 2426 (2018); https://doi.org/10.1364/AO.57.002426
[27] M. A. A. Shafi, S. Sen, Sensing and Bio-Sensing Research 29, 100372 (2020); https://doi.org/10.1016/j.sbsr.2020.100372
[28] K. Ahmed, F. Ahmed, S. Roy, B. K. Paul, M. N. Aktar, D. Vigneswaran, M. S. Islam, IEEE Sensors Journal 19(9), 3368 (2019); https://doi.org/10.1109/JSEN.2019.2895166
[29] M. S. Islam, J. Sultana, K. Ahmed, M. R. Islam, A. Dinovitser, B. W. H. Ng, D. Abbott, IEEE Sensors Journal 18(2), 575 (2017); https://doi.org/10.1109/JSEN.2017.2775642
[30] M. S. Islam, J. Sultana, A. Dinovitser, K. Ahmed, B. W. H. Ng, D. Abbott, Optics Communications 426, 341 (2018); https://doi.org/10.1016/j.optcom.2018.05.030
[31] M. B. Hossain, E. Podder, A. A. M. Bulbul, H. S. Mondal, M. Raihan, M. T. Islam, In 2019 10th International Conference on Computing, Communication and Networking Technologies (ICCCNT) (pp. 1-4), IEEE (2019, July).
[32] M. M. Hasan, S. Sen, M. J. Rana, B. K. Paul, M. A. Habib, G. M. Daiyan, K. Ahmed, In 2019 Joint 8th international conference on informatics, Electronics & Vision (ICIEV) and 2019 3rd international conference on imaging, Vision & Pattern Recognition (icIVPR) (pp. 40-44), IEEE (2019, May).
[33] M. Hossain, E. Podder, Applied Physics A 125(12), 1 (2019); https://doi.org/10.1007/s00339-019-3164-x
[34] M. Rahaman, H. S. Mondal, M. Hossain, M. Ahsan, R. Saha, SN Applied Sciences 2(8), 1 (2020); https://doi.org/10.1007/s42452-020-03210-2
[35] M. S. Islam, J. Sultana, A. Dinovitser, B. W. H. Ng, D. Abbott, Optics Communications 413, 242 (2018); https://doi.org/10.1016/j.optcom.2017.12.061
[36] J. C. Knight, Nature 424(6950), 847 (2003); https://doi.org/10.1038/nature01940
[37] M. De, T. K. Gangopadhyay, V. K. Singh, Sensors 19(3), 464 (2019); https://doi.org/10.3390/s19030464
[38] P. Zhang, J. Zhang, P. Yang, S. Dai, X. Wang, W. Zhang, Optical Fiber Technology 26, 176 (2015); https://doi.org/10.1016/j.yofte.2015.09.002
[39] R. T. Bise, D. J. Trevor, In Optical fiber communication conference (p. OWL6), Optical Society of America (2005, March).
[40] A. Ghazanfari, W. Li, M. C. Leu, G. E. Hilmas, Additive Manufacturing 15, 102 (2017); https://doi.org/10.1016/j.addma.2017.04.001
[41] H. Ebendorff-Heidepriem, J. Schuppich, A. Dowler, L. Lima-Marques, T. M. Monro, Optical Materials Express 4(8), 1494 (2014); https://doi.org/10.1364/OME.4.001494
[42] Fabrication of Photonic Crystal Fibers, Photonic Crystal fiber Science, accessed on 27th August, 2022 [Online]. Available: http://www.mpl.mpg.de/en/russell/research/tdsu-3-fiber-drawing.html